Lithological Discrimination and Structural Trends in W-Rwanda (Africa) on Images of Airborne Radiometric and Aeromagnetic Surveys, Coregistered to a Landsat TM Scene*

M. Fernandez-Alonso
Royal Museum for Central Africa, Tervuren, Belgium
A. Tahon
Bureau of Geological Consultancy S.A. -BUGECO, Bruxelles, Belgium

ABSTRACT: Processing and interpretation of an airborne gamma-ray and aeromagnetic survey, combined with Thematic Mapper imagery, enabled the successful discrimination of lithological units and their geological and structural interpretation in a complex area where weathering and a dense vegetation cover make traditional mapping extremely difficult. The visual inspection of RGB color composites reveals the differentiation of the area into distinct color domains, each of which has been related to existing geologic units. The aeromagnetic data not only reveal superficial structures, but also show deeper structural detail inside the tectonometamorphic complexes of the area, adding weight to existing hypotheses on the evolution of the Kibaran orogeny.

INTRODUCTION

IN RECENT YEARS IMAGE PROCESSING TECHNIQUES, originally developed for analyzing satellite data, have been applied to the analysis of geophysical and geochemical prospecting data. This development led to the recognition that, for these data types, the traditional contour map masks much of the embedded information, in particular, lithological composition and geological structure.

Processed shaded-relief and color composite images have proved to be particularly effective forms of presentation for regional surveys. Color images can contain different information sources combined into a single image, exploiting the inherent ability of the human visual system to interpret intensity (gradient, relief) and textural (color) information (Drury and Walker, 1987).

Shaded-relief presentations, which treat the information as topography (or digital elevation) illuminated from a particular direction, have the additional property of enhancing features which trend roughly perpendicular to the direction of illumination. This technique has the effect of enhancing subtle but often important lineaments which are not apparent on conventional contour maps.

With the advance of computer image processing technology, which has seen much development in the processing and enhancement of satellite imagery such as Landsat (MSS and TM) and SPOT, different methods of displaying and processing geophysical data have been developed. This technology relies on the representation of the data in a digital raster (grid) format which can be displayed on a color computer monitor or plotter as an image containing both amplitude and spatial information. In this form the data may also be statistically analyzed, enhanced for visual inspection, and combined with other types of data into color-composite images.

Many geoscientists have used geophysical data, primarily gravity and airborne gamma-ray spectrometer and aeromagnetic data, to map lithological and structural patterns (Murray *et al.*, 1989; Lee *et al.*, 1990; Fernandez-Alonso and Trefois, 1990). Furthermore, many scientists have applied various image analysis and statistical techniques to manipulate and color-enhance geophysical data in digital raster format (Drury and Walker, 1988; Harris, 1990).

*Presented at the Eighth Thematic Conference on Geologic Remote Sensing, Denver, Colorado, 29 April-2 May 1991.

DATA ACQUISITION AND PREPARATION

In the scope of a cooperative agreement between the Rwandese and Canadian governments, a combined airborne radiometric and magnetometric survey was flown, between June and October 1981, by Sander Geophysics Ltd. (Canada) under the supervision of the Canadian International Development Agency and the Geological Survey of Canada. With the agreement of the Rwandese authorities, the Department of Geology and Mineralogy of the Royal Museum for Central Africa obtained a copy of the data on CCT from the Canadian Geological Survey.

The gamma-ray data were recorded as number of discharges per minute in a SANDER SPM-12 gamma spectrometer, using thallium-doped 33,500cc sodium iodine detectors. Four channels were measured in the following energy windows: total 0.40 to 2.82 MeV, potassium (^{40}K) 1.36 to 1.56 MeV, uranium (^{214}Bi) 1.66 to 1.86 MeV, and thorium (^{208}Th) 2.42 to 2.82 MeV. The data were gathered every second and localized using the inertial navigation system of the helicopter which was calibrated using air photographs and by navigation on sight. The values for the four channels were corrected for variations in flight altitude, for drift, and for the influence of the detector background and Compton effect.

The number of discharges for the Th, U, and K channels were converted to equivalent concentrations (ppm for Th and U, percent for K) taking into account the detectors' characteristics for the measured energy window, the flight altitude, and the time interval between measurements. These equivalent concentrations correspond to the theoretical amount of the element which would produce the detected gamma-ray signal.

The aeromagnetic data were gathered every second by measuring the total intensity of the magnetic field to a precision of 0.10 gamma, as detected by a SANDER NPM-5 nuclear precession proton magnetometer. The measuring points were positioned in the same way as the radiometric data. The total intensity data were corrected for diurnal variations, and the international

0099-1112/91/5709–1155$03.00/0

geomagnetic reference field (1981.5) was subtracted from the intensity data to remove regional effects.

The available satellite imagery for western Rwanda, with an area of about 15,000km², is provided by the adjoining parts of two Landsat-5 Thematic Mapper scenes (path 173/62, quad 2 and path 173/61, quad 4). The scenes used in this research were recorded during the dry season, with a sun elevation of 45° and an azimuth of 55° (WRS).

CREATION OF IMAGES

PREPROCESSING

Landsat-5 Thematic Mapper Band 5 (1550 to 1750 nm) of the two scenes was resampled one pixel for two horizontally and vertically and assembled into a 1598-by 2048-pixel mosaic, with a ground resolution of ± 60 by 60 m, for further integration with the Th, U, and K radiometric data.

For the whole of western Rwanda, the geophysical data comprise a total of 875,680 radiometric and 881,790 aeromagnetic datapoints, theoretically collected every 35 m along flight lines 500 m apart. Every point is localized with its UTM coordinates on the existing 1:100,000-scale topographic maps of the area. To prevent the generation of artifacts due to the anisotropy of the survey, the data files were subsampled using only one out of every five points, resulting in a matrix of 175,136 points in a 175- by 500-m grid.

For every 1:100,000-scale map sheet, the data were regridded to a regular 512 by 512 grid using quadratic spline functions. These gridded files correspond to consecutive ground areas covering ± 110 by 110 m per cell. After regridding, their histogram was rescaled between 0 and 255. This produces four radiometric and one aeromagnetic 512 by 512 byte files ("channels") for every map sheet which can be manipulated in an image processing system. A mosaic covering the whole of western Rwanda was produced for every channel.

The Landsat Thematic Mapper scene and the geophysical data were coregistered to the same UTM reference grid using 50 control points, identified on both the satellite pictures and the topographic maps. The registration of the geophysical data grid (after processing and manipulation) was done with a second-degree model using the nearest-neighbor method.

PROCESSING

The five geophysical "channels" were processed so as to enhance the embedded lithological and structural information.

Total Gamma-Ray and Magnetic Field Intensity Data.

A primary grey-tone image of the total radiometric signal was hill-shaded from west to east using the first vertical derivative filtering (FVD) technique (McGarth *et al.*, 1976; Lee *et al.*, 1990) which consists of applying the following convolution filter to the data:

$$\begin{matrix} -1 & 0 & 1 \\ -1 & 0 & 1 \\ -1 & 0 & 1 \end{matrix}$$

Although not strictly the mathematical equivalent of true artificial illumination, the result is quite similar.

To combine the thematic information of the total gamma ray file with the structural information of its filtered derivative, a color-coded combination of both images was produced. This was achieved by applying an intensity-hue-saturation (IHS) to red-green-blue (RGB) transform using the FVD as I, the total field as H, and a fixed value of 128 as S (50 percent saturation). The resulting image shows the total radiometric signal hill-shaded from the west and color-coded between cyan (low intensity) and magenta, going to purple (high intensity) (see Plate 1 for the color coding).

The manipulation of the total intensity magnetic field data is similar to the one used on the radiometric signal channel. A total magnetic field file and its derivative were combined into an RGB image (Plate 1) in exactly the same way as for the total radiometry.

Th, U, and K Radiometric Data.

From the Th, U, and K data files, an RGB color composite was produced by allocating Th to the red, U to the green, and K to the blue channel after a linear stretch of the channels' histograms. In the resulting image, differences in lithology showed up as different colors and color tonalities. The diffuse structural information was enhanced by a processing sequence exemplified in Figure 1. This manipulation is based on the assumption that the structural information is expressed by local, sometimes abrupt, variations in the radiometric signal, corresponding to the local changes in chemical composition of the substratum (e.g., alternations of quartzitic and pelitic rocks which underline the structure of the area).

In an RGB to IHS transform, the majority of this information must be contained in the Intensity channel. Applying an FVD convolution filter to this channel enhances the high frequency variations of the intensity "topography." After adding this FVD file to the original radiometric data files, an RGB color composite is produced. This image (Plate 2) shows the colored lithological information modulated by its embedded structural information.

Integration of Radiometric Data and Landsat TM Scenes

The Th, U, K color composite was superimposed onto Band 5 of the Landsat-5 TM mosaic, which gives the most topographic detail. This allows the exact localization in the field of the observed radiometric features. The integration of the gamma-ray and the TM channel was achieved by adding half of the DN of TM Band 5 to each of the three radiometric channels. An RGB color composite (Plate 3) was produced by allocating the modified Th, U, and K files, respectively, to the red, green, and blue channel.

GEOLOGICAL SETTING

Rwanda lies in Central Africa surrounded by Uganda, Tanzania, Burundi, and Zaïre. The country was originally covered with tropical rainforest in the higher parts and savannah in the lower areas. Most of the original vegetation has been destroyed due to intensive agriculture, and only some parts subsist in remote or protected areas.

The geology mainly consists of Middle Proterozoic formations with a local Cenozoic cover (Figure 2). Apart from Holocene superficial deposits (alluvium, colluvium), the Cenozoic cover consists of volcanic sequences belonging to the East African Rift system. They are of Tertiary age in the southwest (volcanic plateau of Cyangugu, part of the S. Kivu volcanic province) and of Tertiary to Quaternary age in the northwest (volcanic province of the Virunga chain), where volcanic activity persists to the present day.

The Middle Proterozoic formations belong to the Kibaran belt, which comprises three major lithologic groups: very low- to low-grade arenitic and pelitic metasediments (locally with volcano-sedimentary sequences), large composite granite bodies with minor metasedimentary and basic igneous enclaves, and

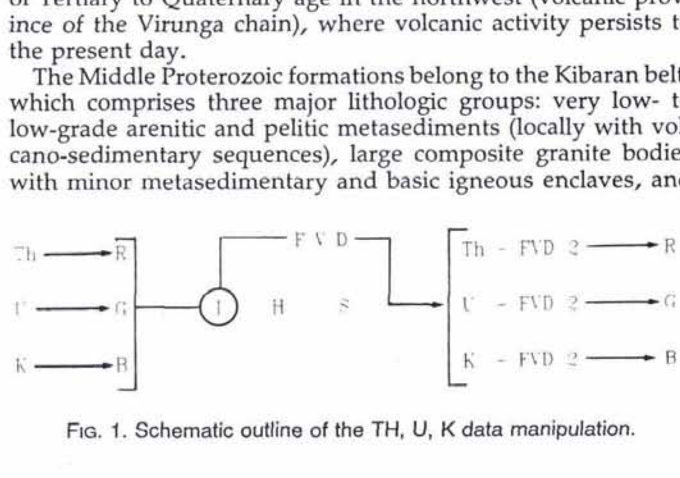

FIG. 1. Schematic outline of the TH, U, K data manipulation.

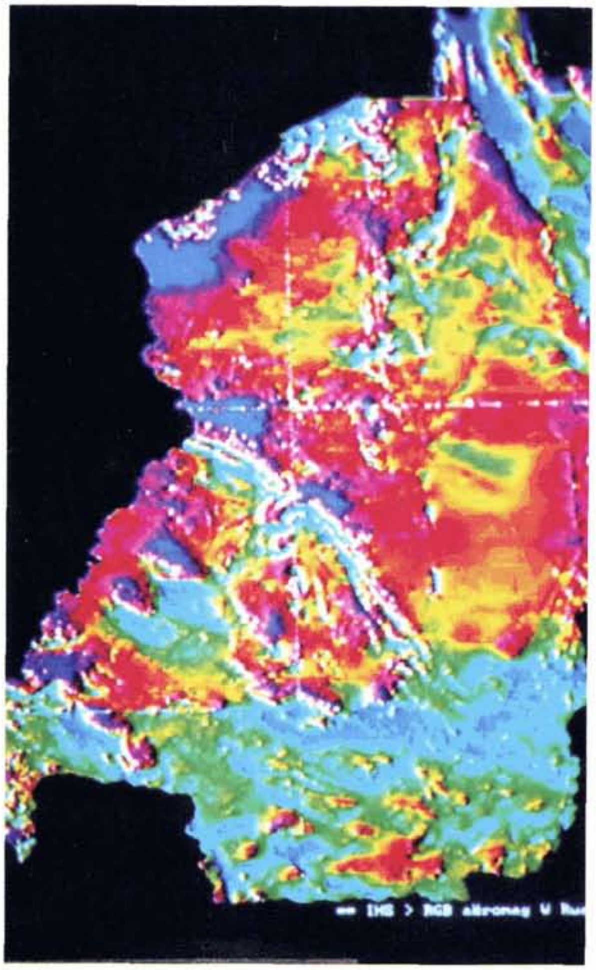

PLATE 1. Hill-shaded color composite of total magnetic field.

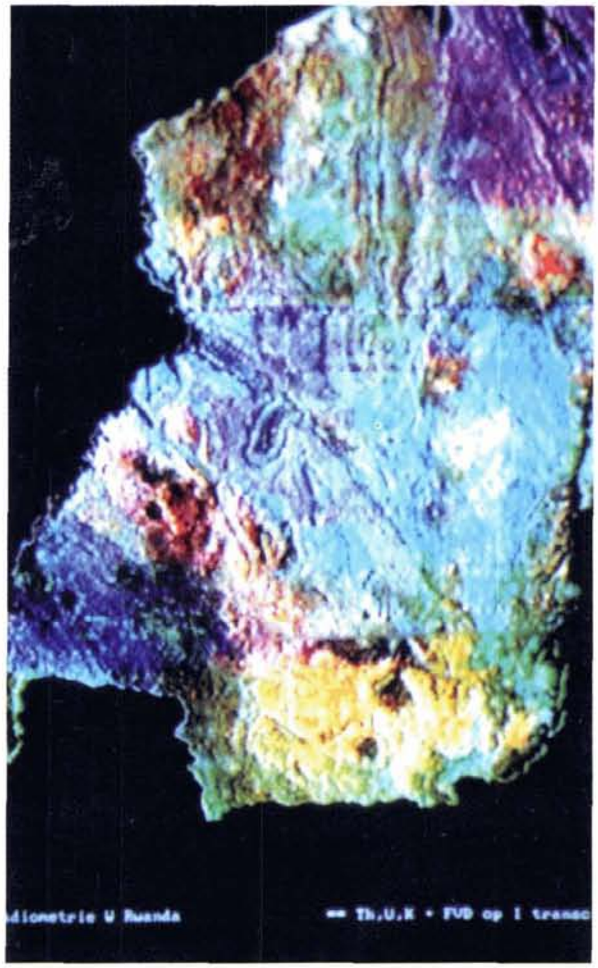

PLATE 2. Hill-shaded color image of Th (red), U (green), and K (blue).

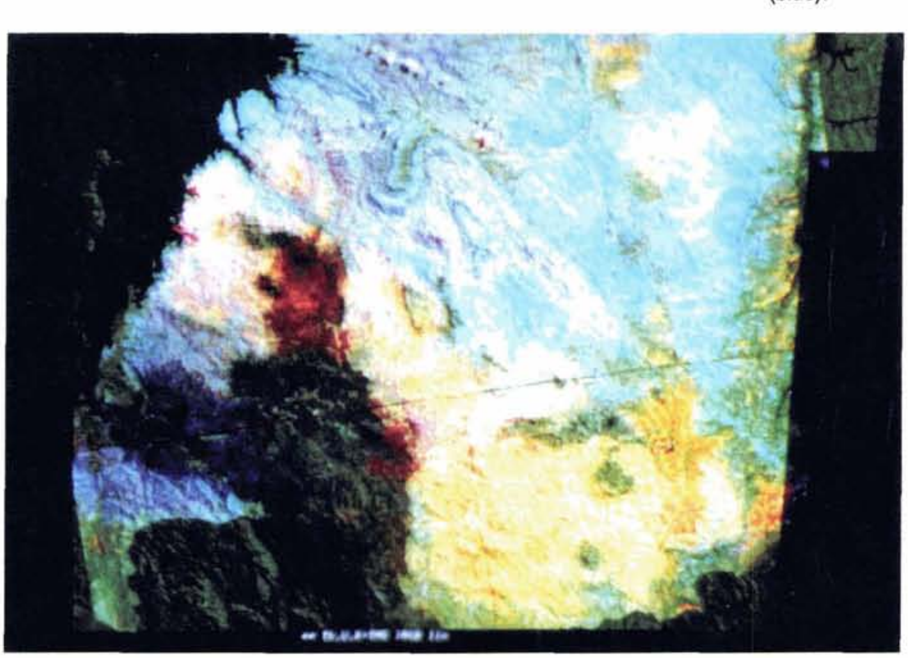

PLATE 3. Color-coded integration of gamma-ray Th, U, and K with Landsat TM5 (Southwest Rwanda).

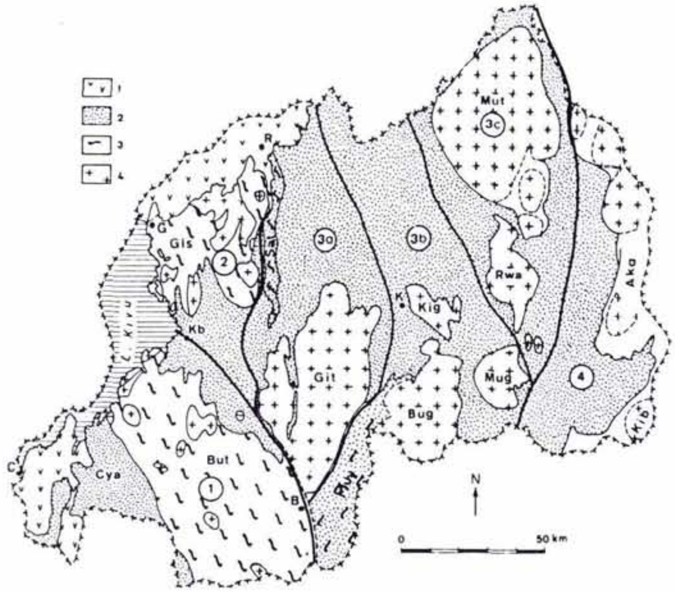

1: Tertiary to Recent lavas; 2: low-grade metasedimentary terrains; 3: granitic-metamorphic complexes; 4: granites. Units: Aka(gera), Bug(esera), But(are), Cya(ngugu), Gis(enyi), Git(arama/Nyabisindu), Kib(ungo), Kig(ali), Mug(esera), Mut(ara), Muy(aga), Rwa(magana), Sat(insyi); Towns: B= Butare, C= Cyangugu, G= Gisenyi, K= Kigali, Kb= Kibuye, R= Ruhengeri

FIG. 2. Structural-lithological units of the Kibaran in Rwanda (circled numbers refer to text).

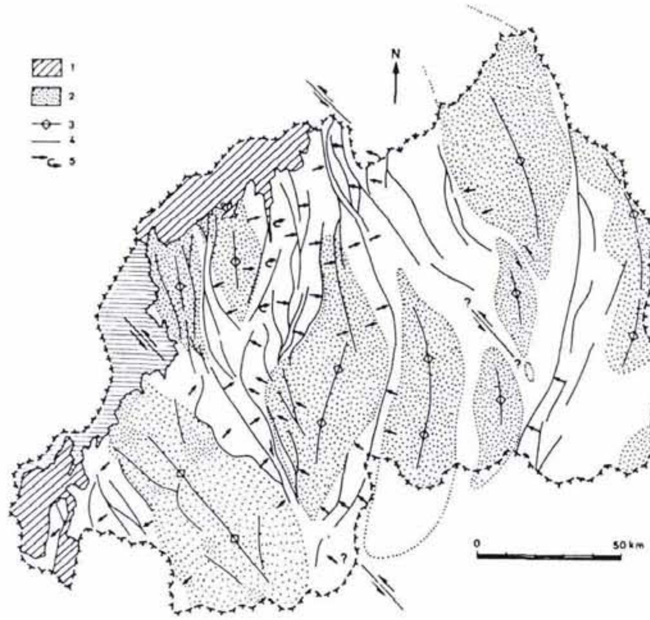

1: Tertiary to Recent volcanics; 2: granitic cores; 3: antiformal axis; 4: faults; 5: vergens of thrusts and folds

FIG. 3. General structural features of the Kibaran in Rwanda.

large complexes of granites, granitic gneisses, and medium-grade metasediments. The sedimentary terrains typically display Appalachian-style folding and thrusting. Trend directions vary from northwest in the western part of the country, to north in the central part, and to northeast in the extreme eastern part. Comparable granite types in Burundi were divided into four generations, dated from 1330 to 1100 Myr (Fernandez, 1987; Klerkx, 1984), which reflect the different stages of the Kibaran orogeny. The main deformation phase is believed to have taken place at around 1180 Myr ago (Klerkx *et al.*, 1987).

The sediments were classified as belonging to the Supergroup of Rwanda (Baudet *et al.*, 1988). Different lithostratigraphic columns were distinguished for east and west Rwanda. The latter is divided from top to bottom into the Rugezi, Cyohoha, Pindura, and Gikoro Groups. The base of the Supergroup of Rwanda has not been observed.

Four major structural units, compartmented by N-S to NW-SE arcuate thrust zones or NW-SE left-lateral shear zones, are distinguished: the granitic-metamorphic Complexes of Butare (SW, no. 1 in Figure 2) and of Gisenyi (NW, no. 2); central Rwanda, consisting of three subunits of granite bodies surrounded by intensely deformed sedimentary terrains (nos. 3a to 3c); and the Akagera-Kibungo area (E, no. 4) separated from central Rwanda by a major N-S thrustfront.

The general pattern of the Kibaran in Rwanda consists of resistant cores, characterized by relatively weak deformation, separated by intensely deformed zones where shear along NW-SE directions and thrusting and folding along general N-S directions occurs. Vergence varies according to the location of the cores. A sketch of the main structural features of Rwanda is reproduced in Figure 3. The picture is reminiscent of the microscopic texture of a mylonitic rock.

Western Rwanda is composed by the complexes of Butare (1) and Gisenyi (2) and the antiformal block of Ruhengeri-Gitarama (3a). The former two display a complex internal structure consisting of low- to medium-grade arenitic and pelitic metasediments, granites, and orthogneisses. The scarcity and poor quality of the outcrops preclude any detailed mapping. The complexes are surrounded by low-grade metasedimentary terrains and the Butare Complex is bordered to the north by a major NW-SE left-lateral shearzone, the Mwogo structure. The Ruhengeri-Gitarama block consists of the Gitarama/Nyabisindu granitic massif forming the core of a large antiformal structure with north-dipping axis. The border with the Complex of Gisenyi is defined by the tectono-metamorphic Complex of Satinsyi (Sat), which corresponds to the core of a north-south synformal structure, heavily mylonitized by intensive thrusting. To the southeast, the Gitarama massif is bordered by the tectono-metamorphic Complex of Muyaga, composed mainly by metasediments of undefinable stratigraphic position and characterized by westward thrusting.

It has been suggested by some authors (Theunissen, 1988, 1989; Tahon, 1990) that the Kibaran D2 deformation was controlled by left-lateral movements along weakness zones in the Lower Proterozoic (Rusizian) basement, under the effect of a regional east-west compressive stress field, the origin of which is still under discussion (Klerkx *et al.*, 1984; Theunissen, 1989). The observed presence of Lower Proterozoic granitic gneisses in the Complex of Butare attests to involvement of the basement (Gerads and Ledent, 1970; Ledent, 1979). The overlying Kibaran sediments would have been passively deformed following a pattern defined by the presence of the resistant nuclei.

LITHOLOGICAL AND GEOLOGICAL INTERPRETATION

LITHOLOGICAL DISCRIMINATION

The RGB Th, U, K color composite, its hill-shaded variant (Plate 2), and its combination with TM Band 5 (Plate 3) were used for the chemical discrimination of the different lithologies. On color hardcopies, the authors manually delineated areas with similar color tonalities, taking into account:

- the obvious color shifts due to changes in calibration of the gamma-ray detectors, particularly for the U channel;
- the damping effect on the radiometric signal by the remnants of tropical rainforest, due to the high moisture content of these areas; and
- the west-east oriented "striping" due to the orientation of flight-lines and the anisotropy of the original data (even after the sub-sampling).

In general, the different rocktypes from the Cenozoic and Precambrain terranes can easily be recognized.

For the Cenozoic, the volcanic rocks of the Virunga province in the north appear in white (= high radiometric content in the three channels), while those of the south-Kivu province display a darkbrownish color (low signal in the three channels). This difference is thought to represent the different chemistry of both provinces; the first being undersaturated sodio-potassic, whereas the second consists of lavas with a tholeiitic and alkalic composition.

For the Middle Proterozoic rocks, the distinction can be made between the sedimentary and crystalline domains: the sedimentary domain appears in green, brown, and purple tones, while the crystalline shows reddish, yellow-orange, and blue tones. Two major and some minor "transitional zones" between the sedimentary and crystalline domains can also be observed.

An important feature is the fact that the different crystalline blocks in the area clearly show a different chemical signature. The Butare and the Gisenyi blocks show a thorium (pink) to thorium-uranium (orange-yellow) rich signature, the latter less clearly due to attenuation of the response by the tropical forest. In contrast, the Nyabisindu block has a high potassic content, shown in blue.

Within the crystalline domain intrusive bodies of contrasting composition can be distinguished quite easily, while the presence of isolated inclusions of sedimentary origin is indicated by darkbrown patches.

A total of 15 different major and minor lithologies have been differentiated. For every lithology, an average equivalent Th, U, and K content was calculated using several polygons in each group and recalculating the mean DN to equivalent concentration (Table 1).

Geological Interpretation

In Figure 4 a simplified lithological map, based on a new lithologic map at 1:250,000-scale for the western half of Rwanda, is presented. This new 1:250,000-scale map was compiled using all the images discussed in this work.

The structural information was extracted from the hill-shaded color images using the most striking linear features. These features mostly correspond to abrupt changes in lithology. Some faults could also be identified as discontinuities and sudden shifts in these lineaments.

In Table 1 the different lithologies have been arranged according to the geological context of the study area. For the Middle Proterozoic rocks in particular, the distinction between the sedimentary and the crystalline domain is quite straightforward.

On the whole, the sedimentary domain is characterized by a lower equivalent concentration in the radiogenic elements Th, U, and K (see the average values in Table 1). The Sed1 unit corresponds to the stratigraphic Gikoro Group, while the Sed2 unit represents the Pindura and Cyohoha Groups. The Sed3 unit does not appear as such on existing geological maps. As it occurs in a relatively inaccessible area covered by tropical forest, it had previously not been identified in Rwanda. It might correspond to the northern extent of Kibaran metasedimentary complexes in northeastern Burundi.

Although of sedimentary signature, the Sed5a and Sed5b units are geologically part of the crystalline domain. The areas occupied by Sed5a are on the margins of the crystalline blocks of Butare and Gisenyi, and most probably correspond to sediments with a locally higher degree of metamorphism. Sed5b is also located on the margin of a crystalline block (Nyabisindu), and is geologically described as the tectono-metamorphic complex of Muyaga. Its radiometric signature, however, shows a great similarity with Sed4, which consists of metaquartzitic enclaves in the granitic rocks of the Butare and Gisenyi blocks.

The signatures of "intrusive" rocks of the crystalline domain have a higher Th, U, and K content than the sediments. Both

Table 1. Equivalent Concentration in Different Lithologies (ppm for Th, U; % for K; av.: mean value of principal lithologies)

	eq.Th	eq.U	eq.K		eq.Th	eq.U	eq.K
	Cenozoic Volcanics				m. Proter.crystalline domain		
cen1	23	9	1.9	cry1	16	4	0.8
cen2	10	4	0.4	cry2	22	5	1.0
				cry3	23	6	0.8
	m.Proter.sedimentary domain			cry4	10	6	1.8
				av.	18.5	5.3	1.0
sed1	15	4	1.1				
sed2	11	4	1.1	cry5	22	7	0.8
sed3	14	7	0.7	cry6	19	8	2.3
av.	12.5	4.5	0.8	cry7	18	4	0.6
				sed4	10	3	0.4
				sed5a	14	6	0.9
				sed5b	11	4	0.5

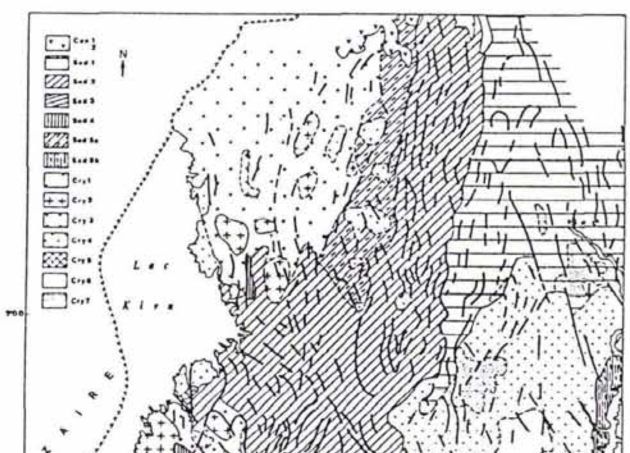

Fig. 4. Simplified lithological map of W-Rwanda (sed. and cry., respectively, sedimentary and crystalline lithology; thick lines: structural lineaments; thin lines: lithological boundaries).

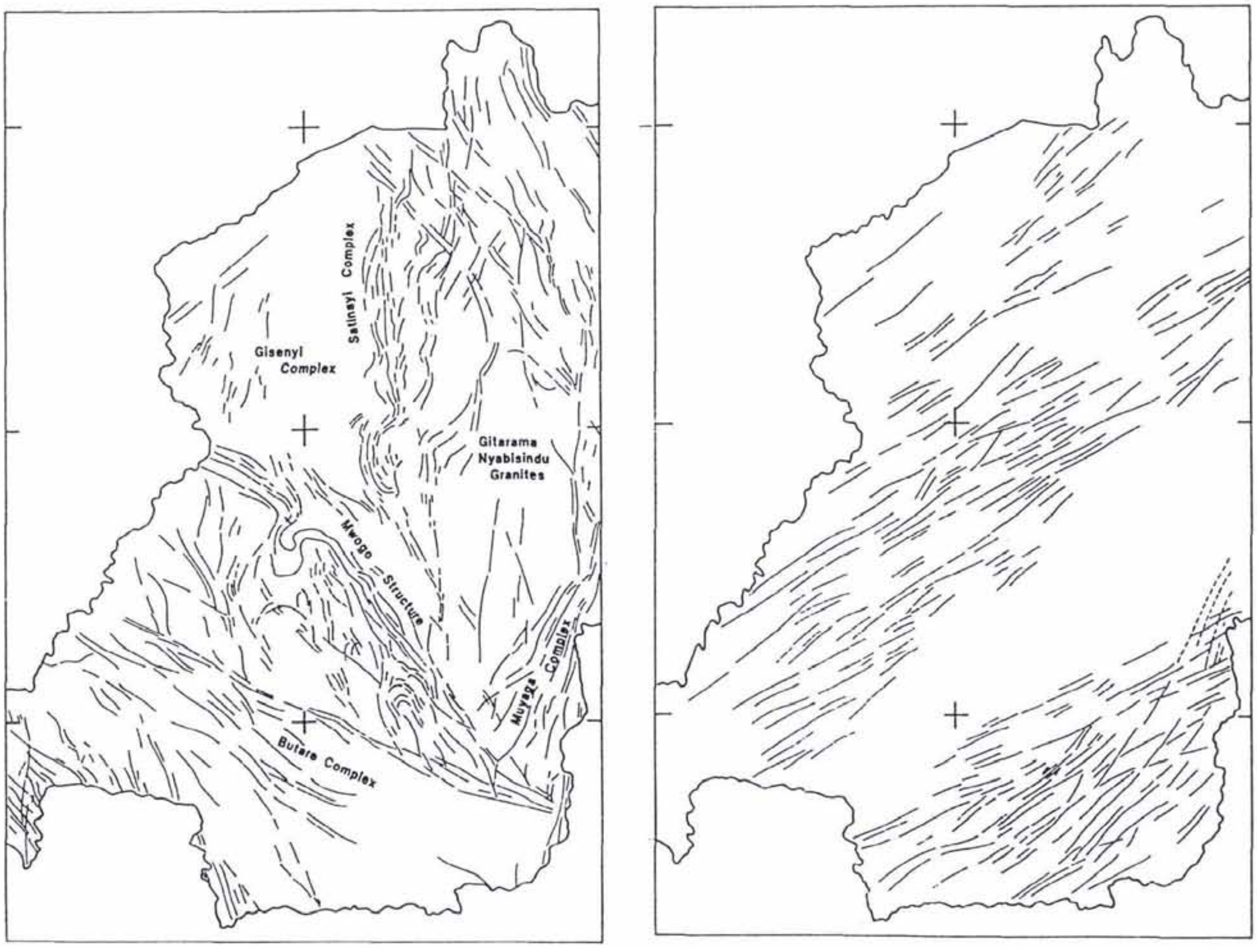

FIG. 5. Lineaments in W-Rwanda, observed on FVD images of total aeromagnetic intensity. (A) Lineaments reflecting main structural pattern. (B) NE-SW cross-cutting lineament set of unknown origin.

Cry1 and Cry3 signatures are interpreted as the expression of the "matrix" of the crystalline complexes, although the presence of those lithologies needs further investigations.

Cry2 and Cry4 represent two different granitic lithologies, both appearing as intrusive bodies in or around the crystalline blocks of Butare and Gisenyi. Cry2 can only be identified within the blocks, whereas the Cry4 intrusive bodies are located on the margins of the blocks and in the surrounding sedimentary rocks. This suggests that there was both a chemical and a spatial controlling factor during their emplacement. The geochemical evolution of these bodies was already studied in the Kibaran terranes of Burundi (Fernandez *et al.*, 1986), but the presence of a spatial relationship is new.

The Nyabisindu crystalline block is apparently totally composed of the Cry4 lithology, and seems to be of a different nature than the Butare and Gisenyi blocks.

Some special signatures within or around the crystalline domain can be observed (Cry5, Cry6, and Cry 7), but their geologic interpretation needs further investigation.

STRUCTURAL ANALYSIS OF THE AEROMAGNETIC IMAGES

A quantitative analysis was carried out by Everaerts (1991) on the aeromagnetic data of the Butare Complex. The present discussion focuses on a qualitative interpretation of the aeromagnetic structures observed on first vertical derivative images (N-S, W-E, NW-SE, and NE-SW gradients). The resulting lineament maps are reproduced in Figures 5A and 5B.

Figure 5A presents a set of NW-SE and N-S lineaments which reflect the main structural pattern as observed in the field (see Figure 3). The sharpest lineaments are formed by (curvi-) linear anomalies occurring in the N-S tectono-metamorphic Satinsyi Complex and along the NW-SE Mwogo structure (see also Plate 1). They correspond most probably to amphibolites, derived from doleritic sills, intercalated in the Gatwaro and Sakinyaga formations. Another set of linear short-wavelength anomalies occurs in the Muyaga Complex in the east. They picture the surface structure as outlined by pyrite-bearing quartzitic mylonite ridges. In the north, very thin, faint NE-SW lineaments appear on the NE-SW gradient image. They represent discontinuities in the "texture" of the local aeromagnetic field and possibly correspond to an important jointset also observed on aerial photographs.

Very few lineaments are present in the Gisenyi Complex, attesting to a relatively homogeneous deep structure without important magnetic surface features. The Butare Complex, on the other hand, is characterized by important NW-SE to WNW-ESE lineaments, almost none of which reflect surface structures. Apart from a number of thin curvilinear anomalies in the SSE prolongation of the Mwogo structure, all of the above lineaments represent discontinuities in the underlying "texture." From comparisons with the known surface geology, it is clear that the aeromagnetic picture over the Butare Complex is shaped by deeper structures, as indicated also by Everaerts (1991). In accordance with the views expressed by Theunissen (1988, 1989) and Tahon (1990), it is believed that the above picture represents internal structures of the Lower Proterozoic Rusizian basement, situated much closer to the surface under the Butare Complex than anywhere else. Depth information may be gathered from a quantitative analysis of the observed anomalies, but this falls outside the scope of the present paper. A major composite WNW-ESE lineament, hereafter referred to as the Butare lineament, runs across the whole of the Butare Complex and cuts off the other NW-SE lineaments. Parallel lineaments occur further south but never attain the same importance.

The following discussion focuses on the interpretation of the Mwogo and Butare data. Figure 6A reproduces a selection of significant photographic and aeromagnetic lineaments in and north of the Butare Complex and Figure 6B presents an interpretation of the large-scale structure of the area.

The thin continuous lines on Figure 6A represent the outcrop traces of the Gatwaro and Sakinyaga quartzites along the Mwogo River valley, the Mwendo synform, and the southward closure of the Satinsyi Complex synform. The fine dashed lines picture the linear aeromagnetic anomalies corresponding to the same formations. In zones 2 and 3 and along the Mwogo River valley, both sets of lines coincide, suggesting the aeromagnetic lineaments are the expression of these trends. Further to the southeast and south-southeast though, the outcrop traces vanish although curvilinear aeromagnetic anomalies persist (zone 4). With surface geology displaying a totally different image (Plate 2), it is believed that the magnetic anomalies represent the subsurface continuation of the Gatwaro and Sakinyaga Formations. Their shape clearly indicates a left-lateral movement pattern, consistent with the regional picture.

The rectilinear trace of the Butare lineament (bold lines) indicates the presence of a major subvertical discontinuity. Considering the general structure of the area and the interpretation presented by Theunissen (1988, 1989), it is suggested that the lineament corresponds to a large subvertical ductile shearzone between two Lower Proterozoic basement blocks, hereafter referred to as the Gisenyi-Nyabisindu block (N) and the Butare block (S). Movement during the Kibaran orogeny was left-lateral and was accompanied by uplift of the Butare block, as suggested by the observed synchronous deformation effects in the overlying Kibaran sediments. Initial sinistral movements along the deep-seated discontinuity occasioned the formation of a large planar dislocation in the overlying metasedimentary terrains, an image of which is presented in Figure 6B. The Mwogo structure would outline the surface trace of this dislocation, two modelized cross-section of which are pictured in Figures 7A and 7B (resp. along lines AA′ and BB′ in Figure 6A). A secundary subvertical shearzone is thought to branch off the Butare lineament south of the Mwendo synform (zone 5, Figure 6A). The pictured continuity of the Mwogo structure to the southeast has been overprinted on the field by the westward thrusting in the Muyaga Complex, thought to belong to a terminal phase of the Kibaran D2 deformation event.

The internal structure of the Butare block would be dominated in the western part by WNW-ESE discontinuities represented by the lineaments in Figure 5A, and in the eastern part by almost W-E aeromagnetic anomalies as observed in Plate 1. The internal structure of the Gisenyi-Nyabisindu block would seem to be mostly masked by overlying Kibaran sediments and granites.

Two major sets of NE-SW lineaments, observed to cut through all existing structures, are pictured in Figure 5B. On the whole, they represent structural discontinuities (faults) rather than independent anomalies. The southeastern set is seen to cut and even displace the W-E anomalies in the Butare block (Plate 1) with apparent sinistral sense. The lineaments to the west, close to Lake Kivu, may actually represent a jointset linked with Recent rift tectonics. The southeastern set of lineaments, however, affects the deeper zones of the Butare Complex and may be of pre-Kibaran origin.

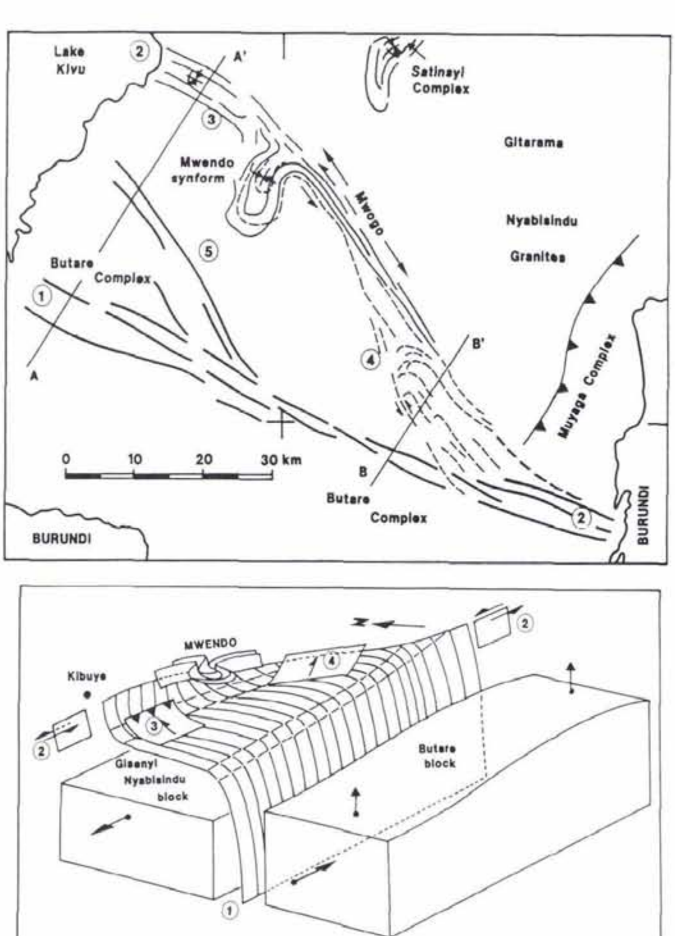

FIG. 6. (A) Compilation of significant lineaments in and north of the Butare complex. Circled numbers refer to Figure 6B and text; AA′ and BB′ indicate cross-sections in Figures 7A and 7B. (B) WSW 3D perspective view of the interpreted subsurface continuation of the Mwogo structure. (1) Ductile sinistral shearzone between Butare block and Gisenyi-Nyabisindu block; (2) NW and SE extremities of the Mwogo structure; (3) indicating component of the NE-ward thrust in the metasedimentary cover, due to uplift of the Butare block; (4) zone with component of E-ward thrust, due to right bend in the sinistral shearzone; (5) secondary subvertical deep shearzone branching off main shearzone.

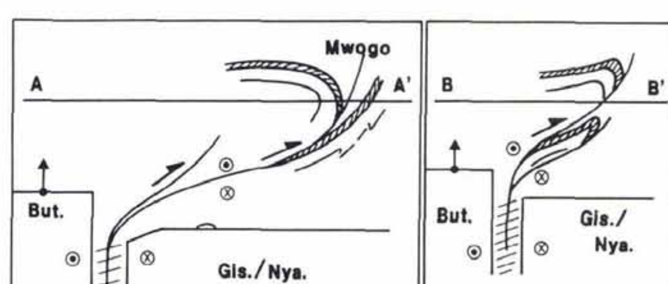

FIG. 7. Modeled sections across the Butare lineament and Mwogo structure. Dotted circles: movement out of the page; crossed circles: movement into the page; shaded bands: structures of the Gatwaro and Sakinyaga formations.

CONCLUSION

The visual inspection of RGB color composite images of the radiometric data and their coregistration with Landsat TM scenes reveals the differentiation of the area into distinct color domains, each of which has been related to existing geologic units. The aeromagnetic data not only reveal superficial structures, but also show deeper structural detail inside the tectono-metamorphic complexes of the area, adding weight to existing hypotheses on the evolution of the Kibaran orogeny.

The use of remotely sensed data to up-date existing geological and lithological maps from areas which are difficult to access provides new opportunities for the growing needs of most African countries to produce detailed and updated maps.

ACKNOWLEDGMENTS

The airborne geophysical data of W-Rwanda were collected and corrected by Sander Geophysics Ltd., Ottawa, and stored in the Geological Survey of Canada. The authors are grateful for these institutions' patience and helpfulness during the elaborate exchange of letters between Canada, Rwanda, and Belgium to provide us with a copy of the data. The approval of the Rwandese government for the use of these data is also gratefully acknowledged. This work is part of a Belgian FKFWO-MI grant to the Department of Geology and Mineralogy of the Royal Museum for Central Africa, for its "Computer Assisted Multi-Data Processing for Geological Mapping" research project.

REFERENCES

Baudet, D., M. Hanon, E. Lemonne, and K. Theunissen, 1988. Lithostratigraphie du domaine sédimentaire de la chaîne kibarienne au Rwanda, *Annales de la Société Géologique de Belgique*, Vol. 112, No. 1, pp. 225–246.

Drury, S. A., and A. S. D. Walker, 1987. Display and enhancement of gridded aeromagnetic data of the Solway Basin, *International Journal of Remote Sensing*, Vol. 8, pp. 1433–1444.

———, 1988. Integration of geological, geophysical and remotely sensed data for the Solway Basin, England, *Proceedings of IGARSS '88 Symposium*, Scotland, 13–16 September 1988, pp. 1663–1666; Ref. ESA SP–284.

Everaerts, M., 1991. *Interprétation de données aéromagnétiques du sud-ouest du Rwanda*, Rapport Annuel pour l'année 1990 du Département de Géologie et de Minéralogie, M.R.A.C. (in preparation).

Fernandez-Alonso, M., J. Lavreau, and J. Klerkx, 1986. Geochemistry and geochronology of the Kibaran granites in Burundi, Central Africa: implications for the Kibaran orogeny, *Chemical Geology*, Vol. 57, pp. 217–234.

Fernandez-Alonso, M., and P. Trefois, 1990. Exploitation geologique de données radiométriques aéroportée, coregistrées avec une scéne Landsat Thematic Mapper, feuille Butare, Rwanda, *Le programme GARS de l'UNESCO/IUGS en Afrique. II: Spectrométrie à haute résolution in situ et analyse d'images LANDSAT et SPOT au Burundi*, (J. Lavreau, editor), Musée Royal de l'Afrique Centrale-Tervuren, Belgique; Annales-Série in-8°, Sciences Géologiques, Vol. 98, pp. 23–38.

Gerards, J., and D. Ledent, 1970. Grands traits de la géologie du Rwanda. Différents types de roches granitiques et premiéres données sur les âges de ces roches, *Annales de la Société Géologique de Belgique*, Vol. 93, pp. 477–489.

Harris, J., 1989. Clustering of gamma-ray spectrometer data using a computer image analysis system, *Statistical Applications in the Earth Sciences* (A. T. Atgerberg, and G. F. Bonham-Carter, editors). Geological survey of Canada, Paper 89–9, pp. 19–31.

Klerkx, J., 1984. Granitoïdes kibariens précoces et tectonique tangentielle au Burundi: magmatisme bimodal lié à une distension crustale. *African Geology* (J. Klerkx and J. Michot, editors), M.R.A.C.-Tervuren, pp. 29–46.

Klerkx, J., J. -P. Liegcois, J. Lavreau, and W. Claessens, 1987. Crustal evolution of the northern Kibaran belt, eastern and central Africa: *Proterozoic Lithospecric Evolution* (A. Kröner, editor), Geodynamic Series, American Geophysical Union, Vol. 17, pp. 217–233.

Ledent, D., 1979. Données géochronologiques relatives aux granites Kibariens du Shaba du Rwanda, du Burundi et du SW Uganda, *Rapport Annuel pour l'année 1978 du Département de Géologie et de Minéralogie*, M.R.A.C., pp. 97–99.

Lee, M. K., T. C. Pharaoh, and N. J. Soper, 1990. Structural trends in central Britain from images of gravity and aeromagnetic fields, *Journal of Geological Society*, London, Vol. 147, pp. 241–258.

McGarth, P. H., L. J. Kornik, and S. D. Dods, 1976. A method for the compilation of high quality calculated first vertical derivative aeromagnetic maps-project 680121, *Report of Activities, part C;* Geological Survey of Canada, Paper 76-1C, pp. 9–17.

Murray, C. G., E. Scheibner, and R. N. Walker, 1989. Regional geological interpretation of a digital coloured residual Bouger gravity image of eastern Australia with a wavelength cut-off of 250 km, *Australian Journal of Earth Sciences*, Vol. 36, pp. 423–449.

Tahon, A., 1990. The Kibaran structural pattern in Rwanda as the result of major lateral shear *Proceedings of the 15th Coll. Afr. Geol.*, Nancy, September 1990.

Theunissen, K., 1988. Kibaran thrust fold belt (D1-2) and shear belt (D2), *IGCP Newsletter*, Vol. 255, No. 1, pp. 55–64.

———, 1989. On the Rusizian basement rise in the Kibara belt of northern Lake Tanganyika. Collision belt geometry or restraining bend emplaced in the Late Kibaran strike-slip environment, *IGCP newsletter*, Vol. 255, No. 2, pp. 85–92.

Theunissen, K., M. Fernandez-Alonso, and M. Hanon, 1988. *Carte Geologique du Rwanda, minute au 1/250,000*, Project Carte Géologique du Rwanda, M.R.A.C., Tervuren-MINIMART Rwanda 1987–1988.